First microwave generation in the FOM free-electron maser

1998 Plasma Phys. Control. Fusion 40 A139

(http://iopscience.iop.org/0741-3335/40/8A/011)

Plasma Phys. Control. Fusion **40** (1998) A139–A156. Printed in the UK PII: S0741-3335(98)92970-0

First microwave generation in the FOM free-electron maser

A G A Verhoeven†‖, W A Bongers†, V L Bratman‡, M Caplan§, G G Denisov‡, C A J van der Geer†, P Manintveld†, A J Poelman†, J Pluygers†, M Yu Shmelyov‡, P H M Smeets†, A B Sterk† and W H Urbanus†

† FOM-Instituut voor Plasmafysica 'Rijnhuizen', Association EURATOM-FOM, PO Box 1207, 3430 BE Nieuwegein, The Netherlands

‡ Institute of Applied Physics, Nizhny Novgorod, Russia

§ Lawrence Livermore National Laboratories, Livermore, CA, USA

Received 23 January 1998

Abstract. A free-electron maser (FEM) has been built as a pilot experiment for a millimetre-wave source for applications on future fusion research devices such as ITER, the International Tokamak Experimental Reactor. A unique feature of the Dutch fusion FEM is the possibility to tune the frequency over the entire range from 130 to 260 GHz at an output power exceeding 1 MW. In the first phase of the project, the so-called inverse set-up is used. The electron gun is mounted inside the high-voltage terminal. The entire beam line was tested successfully with extremely low loss current, lower than 0.05%. The first generation of millimetre waves was achieved in October 1997. The highest peak power measured so far is 700 kW at 200 GHz. This was achieved with a beam current of 8 A and an acceleration voltage of 1.77 MV. The output power, start-up time and frequency correspond well with the simulation results. The parameter scans for the longitudinal undulator gap, acceleration voltage and reflection coefficient have given a wide range of interesting data of which a few highlights are given.

1. Introduction

A free-electron maser (FEM) has been built as a pilot experiment for a millimetre-wave source for applications on future fusion research devices such as ITER, the International Tokamak Experimental Reactor [1]. A unique feature of the Dutch fusion FEM is the possibility to tune the frequency over the entire range from 130 to 260 GHz at an output power exceeding 1 MW.

The system consists of a 12 A thermionic electron gun and a 2 MeV electrostatic acceleration. The undulator and millimetre-wave system are located inside a terminal at 2 MV level. The terminal is placed inside a steel vessel of 11 m length and a diameter of 2.6 m, filled with SF_6 at 7 bar. After interaction with the millimetre waves in the undulator, the energy of the spent electron beam is recovered by means of a decelerator and a multi-stage depressed collector. This approach is expected to lead to an overall system efficiency of 50% [2].

For long-pulse generation a low-loss current, lower than 20 mA is essential. Therefore, the electron beam line is entirely straight from gun to collector. The millimetre waves are directed sideways from the electron beam, by means of a stepped waveguide. This is a

‖ E-mail address: verhoeven@rijnh.nl

0741-3335/98/SA0139+18$19.50

symmetrical step in the transverse dimension of a low-loss HE_{11} waveguide. Furthermore, an adjustable reflector enables adjustment of the feedback power.

In the first phase of the project, a so-called inverse set-up is used. In this phase, the electron gun is mounted inside the high-voltage terminal at -2 MV. The undulator and waveguide system are outside the pressure vessel at ground potential for easy adjustments and fine tuning of the entire system. Consequently, the decelerator and depressed collector cannot be used yet. This means that the entire electron beam has to be supplied by the -2 MV power supply. This results in a very fast change of its voltage level and therefore the FEM pulses are limited to 10–20 μs.

2. Application of a FEM to ITER

A free-electron maser combines the advantages of high-power, high-frequency millimetre-wave sources for electron cyclotron wave (ECW) applications, such as gyrotrons, with the additional advantages of continuous tunability, a higher frequency and (eventually) a higher power per unit. The specifications for the fusion FEM are optimized for applications to ITER. At this moment a total additional heating power of 100 MW is foreseen for ITER, of which, most probably, 50 MW will be supplied by ECW sources.

The frequencies (130–260 GHz) are chosen such that for ITER (with a toroidal magnetic field of up to 5.7 T on-axis) both fundamental on-axis heating at 170 GHz and off-axis heating between 140 and 200 GHz can be achieved. Furthermore, the ideal frequencies for electron cyclotron (EC) current drive are from 220 to 260 GHz. The FEM is constructed in such a way that it can be used for start-up at frequencies beginning at 130 GHz. In addition, the same installation can be tuned within 1 min to again give over 1 MW of power for heating or current drive at any desired plasma position. The specifications can be modified at any time to meet other requirements.

Now, a maximum pulse length of 100 ms is foreseen. The major modification from the current project to a FEM for application on ITER is to extend the pulse length to CW. Furthermore, since a total ECW power of 50–100 MW is foreseen, we have studied an upward scaling of the power per unit from 1 MW to 4 or 5 MW and the conclusion of the study is that it is feasible [3]. Compared to fixed-frequency or stepwise frequency tunable high-power sources, a source with a continuously adjustable frequency has a number of additional advantages.

- All magnetic flux surfaces in the plasma can be reached without changing the toroidal magnetic field, so without changing the target plasma.
- For $m = 2$ mode stabilization the variations in the q profile can be followed by tuning the absorption region to the change of the $q = 2$ radius. Furthermore, now a broadening of the deposition layer, because of a toroidal deflection of the beam, can be avoided.
- Fine control over breakdown location is possible in the case of pre-ionization by electron cyclotron heating (ECH) and ECH-assisted start-up.
- ECH can control edge localized modes by changing the resonance location.
- A simple, small and rigid waveguide launcher can be used, whereas in the case of a fixed-frequency source a launcher with a rotatable mirror at variable angles is needed.
- Current drive is easier to apply and can be more efficient, since the absorption region can be chosen more accurately.
- Electron transport barriers can be manipulated dynamically in a very elegant way by scanning the deposition area [4].
- Disruptions can be avoided more efficiently by choosing the deposition area carefully.

3. Basic layout

The basic layout of the FEM is largely determined by the requirement for high overall efficiency. This together with fast tunability and CW operation determines the choice for a DC acceleration and deceleration system rather than an RF system. The choice for a maximum electron energy of 2 MeV and a beam current of 12 A has been made on the basis of simulations of the interaction between the electron beam and the millimetre waves. The main parameters of the fusion FEM are given in table 1. The required high system efficiency demands an efficient recovery of the spent electron beam leaving the undulator. For this purpose a decelerator and a depressed collector are incorporated. This results in the basic layout of the fusion FEM as shown in figure 1.

Table 1. Design parameters of the fusion FEM.

Millimetre-wave frequency	130–260 GHz
Millimetre-wave output power	1 MW
Electron energy	1.35–2 MeV
Electron beam current	12 A
Electron loss current	< 20 mA
Normalized beam emittance (xx')	$\pm 20\pi$ mm mrad
Pulse length	100 ms
Overall efficiency (mains to P_{MMW})	$> 50\%$
Waveguide mode	HE_{11}
Type of waveguide	Rectangular, corrugated
Cross section of primary waveguide	15×20 mm^2
Separation MMW beam, electron beam via	stepped waveguides
Undulator period	40 mm
Undulator gap	25 mm
Peak undulator field, section 1	0.2 T
Number of full cells, section 1	20
Gap between undulator sections	35–65 mm (adjustable)
Peak undulator field, section 2	0.16 T
Number of full cells, section 2	14
Total number of cells (incl. matching)	38
Length of undulator	1.58 m

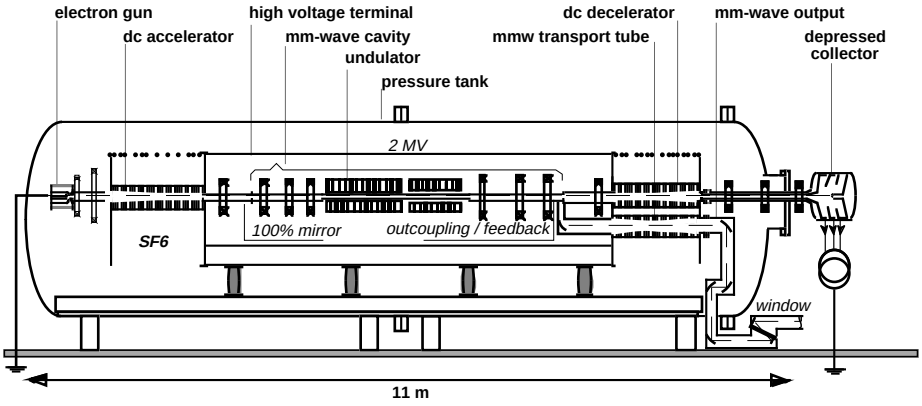

Figure 1. Schematic layout of the fusion FEM.

The undulator and the millimetre-wave system are located at a high-voltage level, in order to enable us to locate both the high-voltage power supplies for the cathode of the electron gun at earth potential, and the electrodes of the depressed collector at low voltages. The power supplies that are connected to the collector, with a total current of 12 A, are located outside the pressure tank at earth potential, while components that need little or no power are inside the high-voltage terminal. Furthermore, the 2 MV high-voltage power supply only has to supply the loss current of 20 mA (maximum). This is because all electrons that pass through the undulator, lose a bit of their energy (just about 5–10% on average) and then go straight on. So they still have an energy close to 2 MV and can travel all the way down from 2 MV to around 100–200 kV (on average). The 2 MV now only has to supply the loss current, just a few mA as we have measured. So a big capacitor with a small load current is sufficient. The 'low' voltage supplies (at 250, 170 and 50 kV) each have to be capable of supplying around 6 A maximum, so these are quite large supplies, but at a moderate voltage level.

4. Simulation of the interaction between electron beam and millimetre waves

The interaction between the electron beam and the millimetre waves inside the fusion FEM has been simulated using several codes. At the start of the project, mostly the CRMFEL (cyclotron resonance maser free-electron laser) code was used, later on the general particle tracking (GPT) code was introduced [5]. CRMFEL is a fully three-dimensional (3D), nonlinear, general-purpose particle-pusher code. Until recently these simulations were done

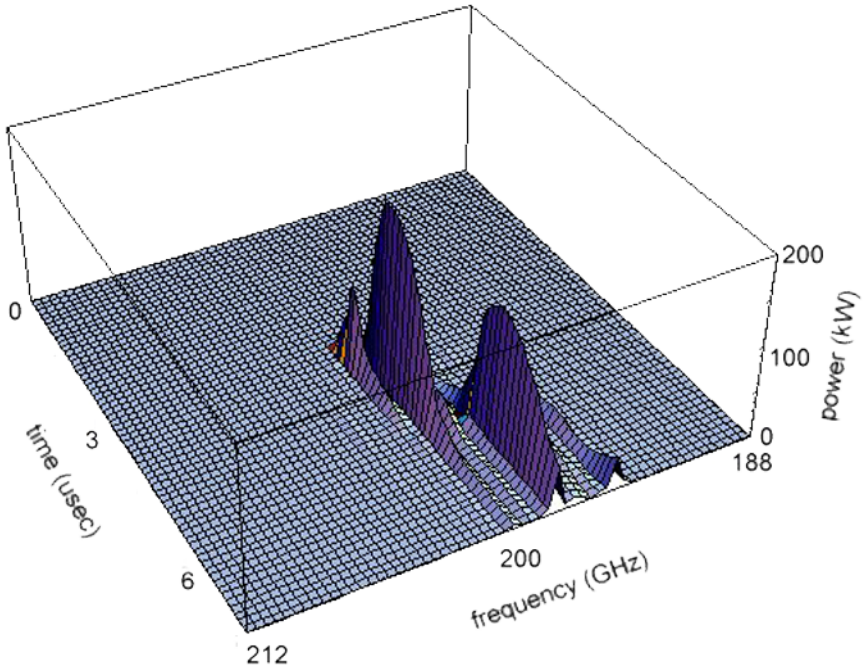

Figure 2. Frequency spectrum as calculated by the Malt 1D code [6]. The beam current is 6 A, the voltage drop is 6 kV μs^{-1}. The acceleration voltage starts at 1.75 MV. Measured data for millimetre-wave reflection and transmission coefficients are taken into account. The beam radius is 1.8 mm. At these parameters it can be noted that a second frequency starts later.

with a single-frequency, stationary version of this amplifier code [6, 7]. Simulations for three different energies indicated that for a 12 A beam the net millimetre-wave power generated is above 1 MW for all frequencies between 130 GHz (at 1.35 MeV) and 260 GHz (at 2 MeV).

The undulator consists of two sections with a different magnetic field. In the first undulator section the net millimetre-wave power (i.e. the total power minus the injected feedback power of around 400 kW) grows to 700 kW at 200 GHz and saturates at the end of the first undulator section. In the second undulator section the electron energy, which is now lower due to the interaction with the millimetre waves, matches the lower undulator strength and the millimetre-wave power grows to 1.3 MW, saturating at the end of the second undulator section. The parameters are optimized in such a way that the electronic efficiency is rather low, of the order of 5–10%, to enable a low-energy spread in the spent electron beam and therefore a high collector efficiency.

Simulations with a modified non-stationary (space-charge included) code developed at the University of Maryland indicate that a parameter regime can be found with a pure single-frequency operation, without any sidebands. The reflection coefficient of the millimetre waves, the size of the electron beam and especially the distance between the two undulator sections have a strong effect on the FEM behaviour [8, 9]. A result of a simulation with this code is given in figure 2. Parameters are very similar to those used during the first experiments, including the time behaviour of the acceleration voltage.

In the mean time, a fully 3D multifrequency FEM (MFF) code, has been developed at Rijnhuizen [10]. The code is based on a multi-frequency model in the continuous beam limit with a 3D description of the electron beam. Space-charge forces are included by a Fourier expression.

5. Millimetre-wave system

The FEM is configured as a millimetre-wave oscillator, consisting of a waveguide amplifier section (inside the undulator) and a feedback and outcoupling system. Since the electron beam line is completely straight the millimetre waves have to be coupled out sideways.

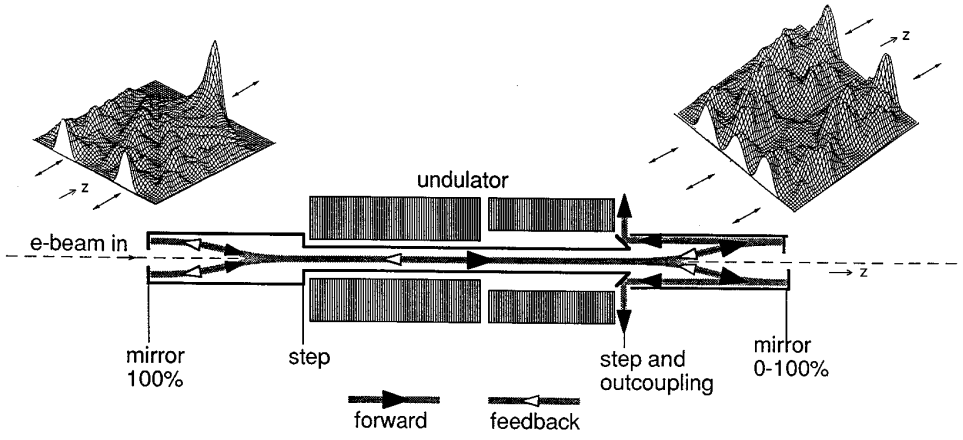

Figure 3. Sketch of the millimetre-wave system. Left of the undulator the 100% reflector and on the right-hand side of the undulator the splitter system is given. This separates the feedback power (going through the primary waveguide back to the 100% reflector) from the output power.

Furthermore, the fraction of the electron current intercepted in the millimetre-wave system should be as small as possible, which means that there should be enough transverse space for the electron beam. After taking all requirements into account a rectangular corrugated waveguide was chosen, carrying the very low-loss hybrid mode HE_{11}, with the E-field parallel to the broad side of the waveguide [11].

Outcoupling and reflection systems are realized through a stepped waveguide, as follows. Both before and after the undulator the transverse cross section of the waveguide changes stepwise from 15×20 mm^2 to 60×20 mm^2 (for a frequency of 260 GHz), where the 60 mm direction is parallel to the undulator magnetic field. This ensures that the primary HE_{11} mode is fully separated into two off-axis beams. These beams have identical profiles and plane wavefronts.

Full separation of the beams takes place after a distance $L = a^2/n\lambda$ from the step, where a is the height of the waveguide after the step and n is the number of parallel beams, respectively [12]. At the position of full separation two mirrors are placed, which reflect the two millimetre-wave beams, while the electron beam passes on-axis through the opening between the mirrors, see figure 3. On the left-hand side simulation results show the field intensities of an HE_{11} beam, propagating in a stepped waveguide. Here it splits into two identical beams. The two beams merge into one HE_{11} beam after reflection on the two mirrors. In this way the 100% reflector is formed. The power in the aperture is < -30 dB.

Outcoupling and feedback of the millimetre waves is realized by a similar stepped waveguide behind the undulator. By giving one of the two mirrors a small displacement in the z-direction, the reflected beams have a phase difference and one on-axis and two

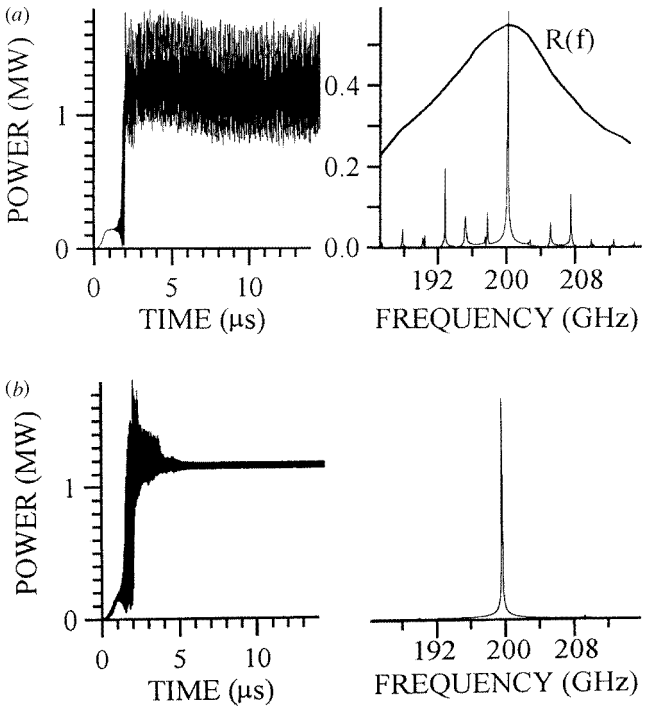

Figure 4. Results of spatio-temporal simulations without (*a*) and with (*b*) account of the frequency dispersion of the feedback, see (*a*) [14].

off-axis backward-propagating beams are formed. By variation of the phase difference, i.e. by translating one of the mirrors, the reflected on-axis power can be varied from 0 to 100% of the generated millimetre-wave power. The on-axis beam propagates back all the way through the primary waveguide. In this way, part of the millimetre-wave power is fed back. The two off-axis beams are coupled out by way of 90° miter bends. On the right-hand side of figure 3 simulation results can be seen for the outcoupling system. In a similar way, the two output beams are merged into one beam in a combiner system that is mounted in parallel to the described beamsplitter system. For a given amplitude feedback the phase of the feedback power is fixed. This means that only at sharp frequencies, spaced about 30 MHz apart, is the phasing exactly correct. So this gives an output spectrum with frequencies 30 MHz apart. On the output side, in the combiner part the phase difference of the two output beams is adjusted by shifting the double-miter bend over a small distance.

Without changing any of the dimensions a fast tunability around the chosen central frequency can be achieved by varying only the electron energy, The full-width half-maximum frequency range is around 4%. However, to adjust the frequency over the entire

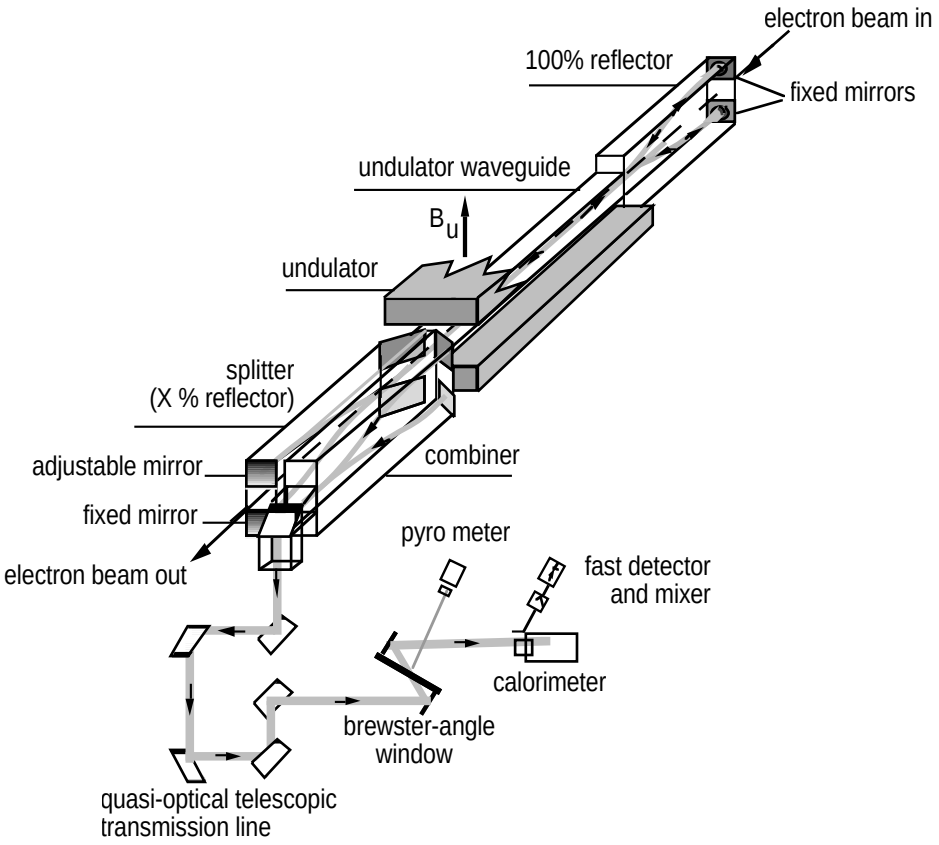

Figure 5. Schematic layout of the millimetre-wave system of the fusion FEM project. On the upper right-hand side is shown the 100% reflector, then the primary waveguide inside the undulator and the combiner. In the combiner the two output millimetre-wave beams from the splitter are combined into one output beam. This single output beam is coupled out via a confocal telescope quasi-optical mirror system.

frequency range of 130–260 GHz, it is necessary to make a variation of a, the height of the stepped waveguide. The sidewalls of the splitter can be adjusted in order to optimize the height from $a = 60$ mm for a frequency of 260 GHz to $a = 85$ mm for 130 GHz.

The frequency dependency of the millimetre-wave feedback coefficient [13] plays an important role in the width of the output frequency spectrum, as can be seen in figure 4. This enables a very small bandwidth at a fixed acceleration voltage [14].

By using a quasi-optical confocal mirror system the single millimetre-wave beam is transferred from the 2 MV load through an insulator tube to ground potential. This is a tube very similar to the acceleration and decelerator tube.

Since the frequency of the FEM has to be varied over a very wide frequency range, it is necessary that the vacuum barrier window is broadband as well. We have chosen a window at the Brewster angle, since this is the only possibility with a bandwidth of an octave. For the first stage of the fusion FEM project a single-disc, edge-cooled boron-nitride Brewster-angle window with a diameter of 140 mm can withstand pulses of at least 100 ms, see figure 5.

6. First experimental results

The first experiments are done in the inverse set-up, where the electron gun is mounted inside the high-voltage terminal and the undulator and waveguide systems are outside the

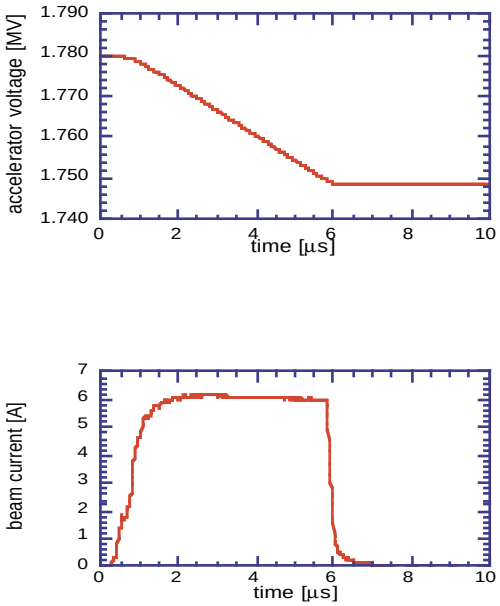

Figure 6. For a pulse with a very pure spectrum the following signals are given: the acceleration voltage (first plot), the beam current (second plot) and the millimetre-wave power as measured by a fast broadband detector (third plot). Furthermore, the millimetre-wave power versus time is given as measured by a narrowband heterodyne system, with a local oscillator frequency of 200.54 GHz (fourth plot). In the final plot the FFT frequency spectrum is given for the frequency difference between the local oscillator and the measured signal. It can be seen that the spectrum is very pure. Acceleration voltage at start, 1.780 MV; feedback coefficient, 0.35.

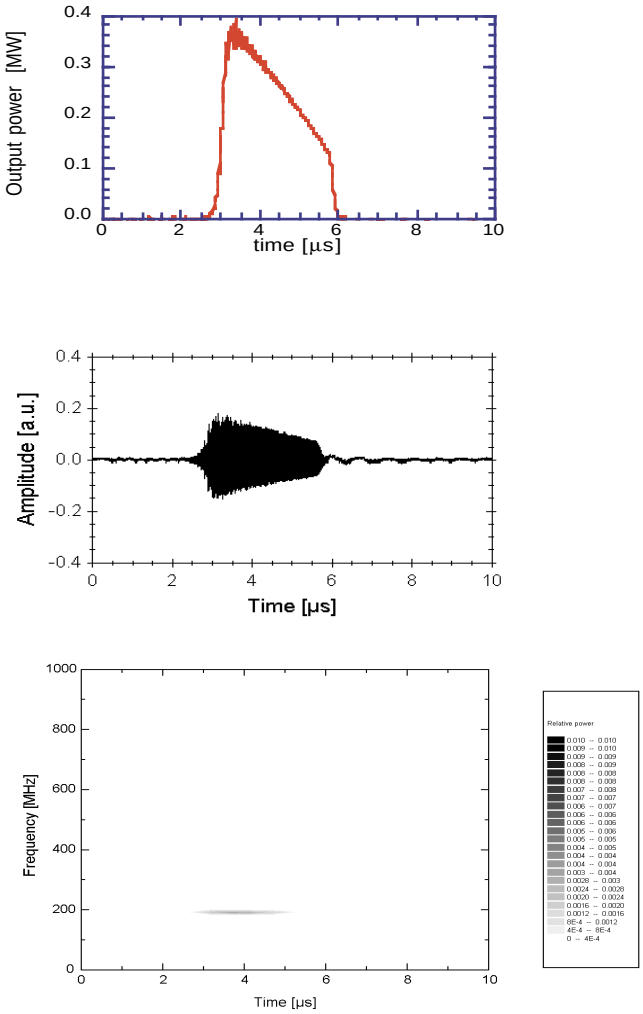

Figure 6. Continued.

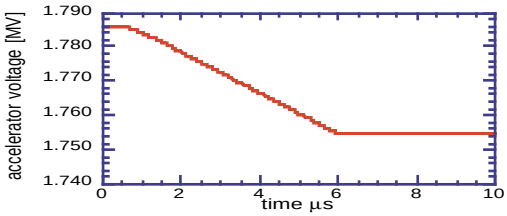

Figure 7. For a pulse with a very broad spectrum (the same signals are given as in figure 6). The local oscillator frequency is 200.04 GHz. It can be seen that the spectrum is much broader now. Acceleration voltage at start, 1.786 MV. Feedback coefficient, 0.35.

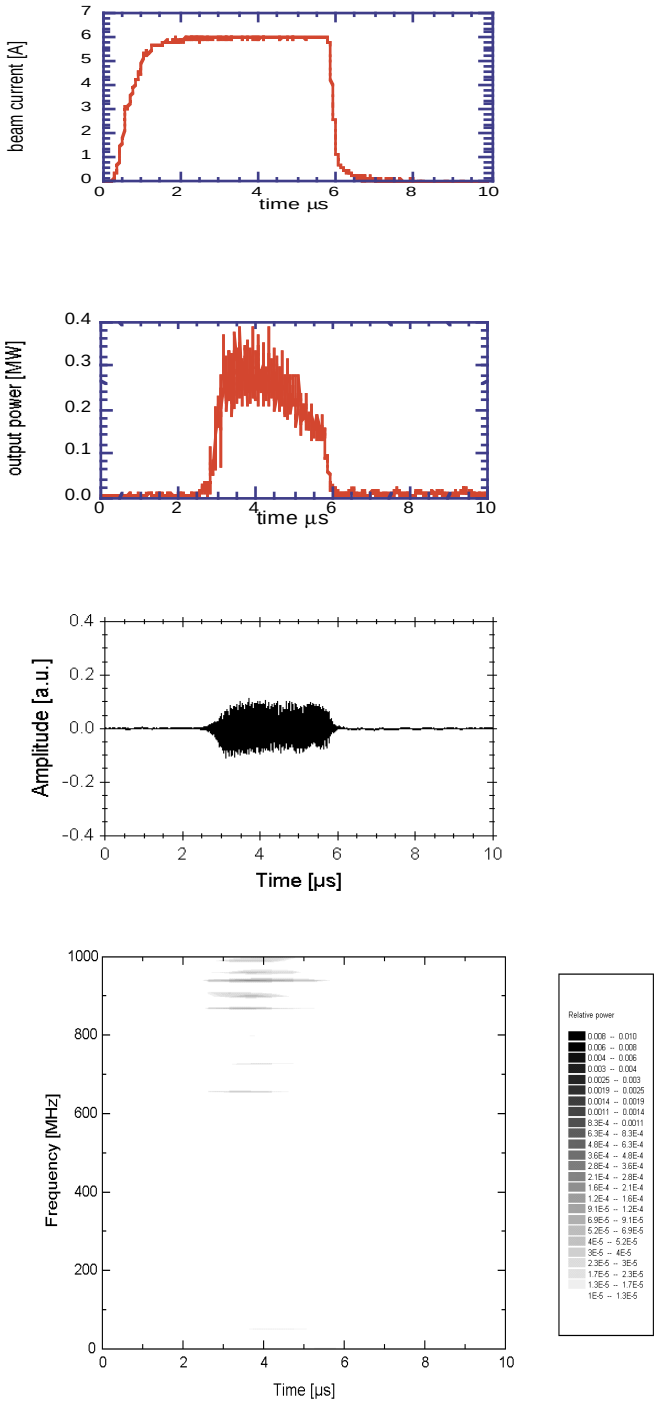

Figure 7. Continued.

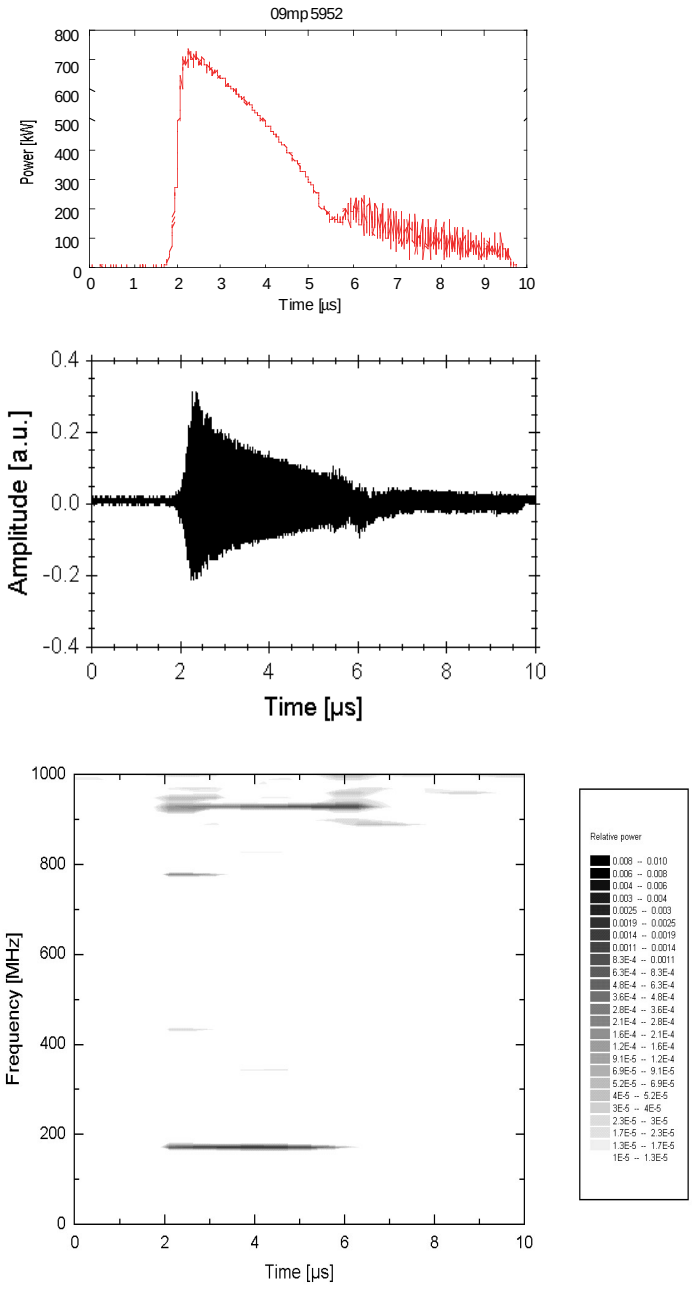

Figure 8. Highest power achieved so far, reaching just over 700 kW. In the frequency spectrum we see at the top a nicely decaying signal at a frequency differing by about 200 MHz from the local oscillator signal, see the lower part of the figure. After around 5 μs the frequency jumps to a lower frequency around 1 GHz from the local oscillator frequency, after 6 μs the frequency drops further, outside the frequency band of ± 1 GHz from the local oscillator frequency of 205.4 GHz. Acceleration voltage at start, 1.77 MV. Feedback coefficient, 0.6. Beam current 8 A.

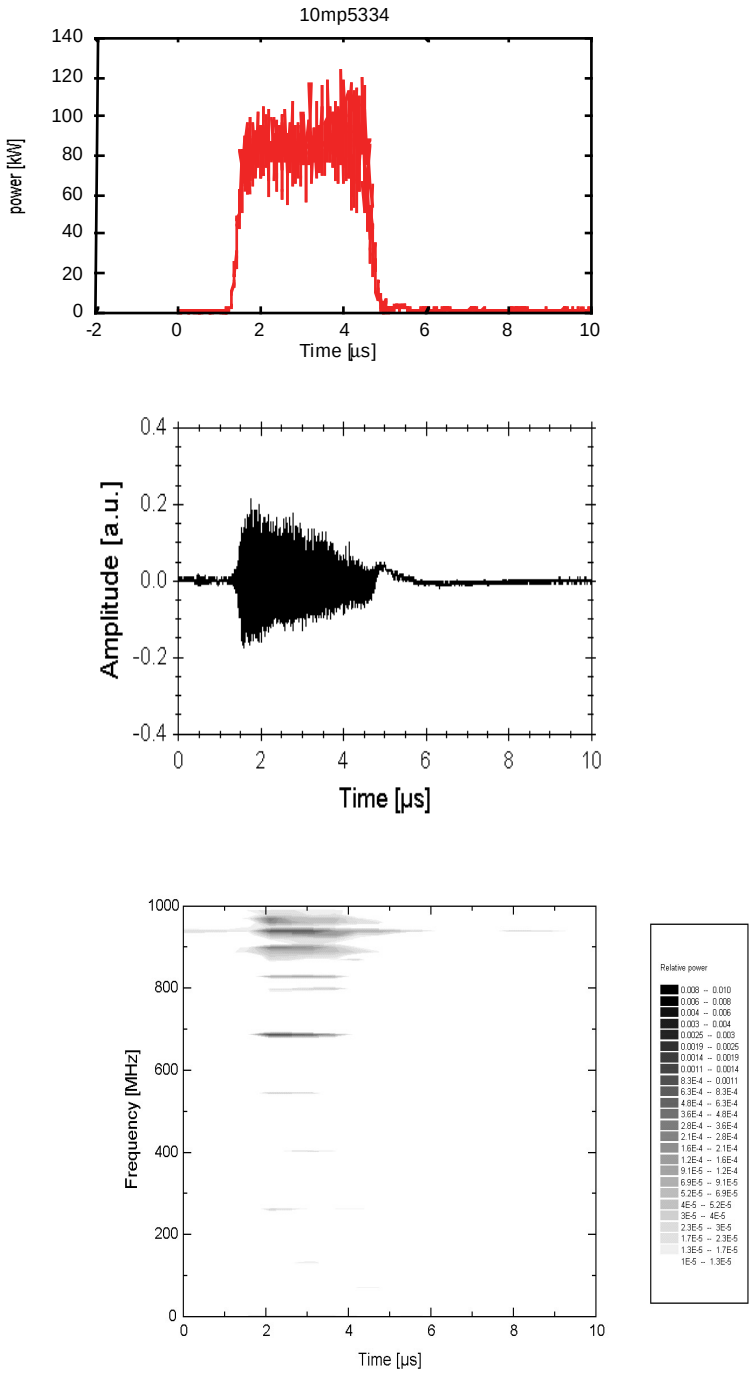

Figure 9. A more or less flat output power signal can be achieved if an increasing signal at a lower frequency is added to the usual decaying signal. In this case the decaying power is composed of a number of frequencies 0.7–1 GHz apart from the local oscillator frequency of 205.4 GHz. Acceleration voltage at start, 1.76 MV. Feedback coefficient, 0.7. Beam current, 6 A.

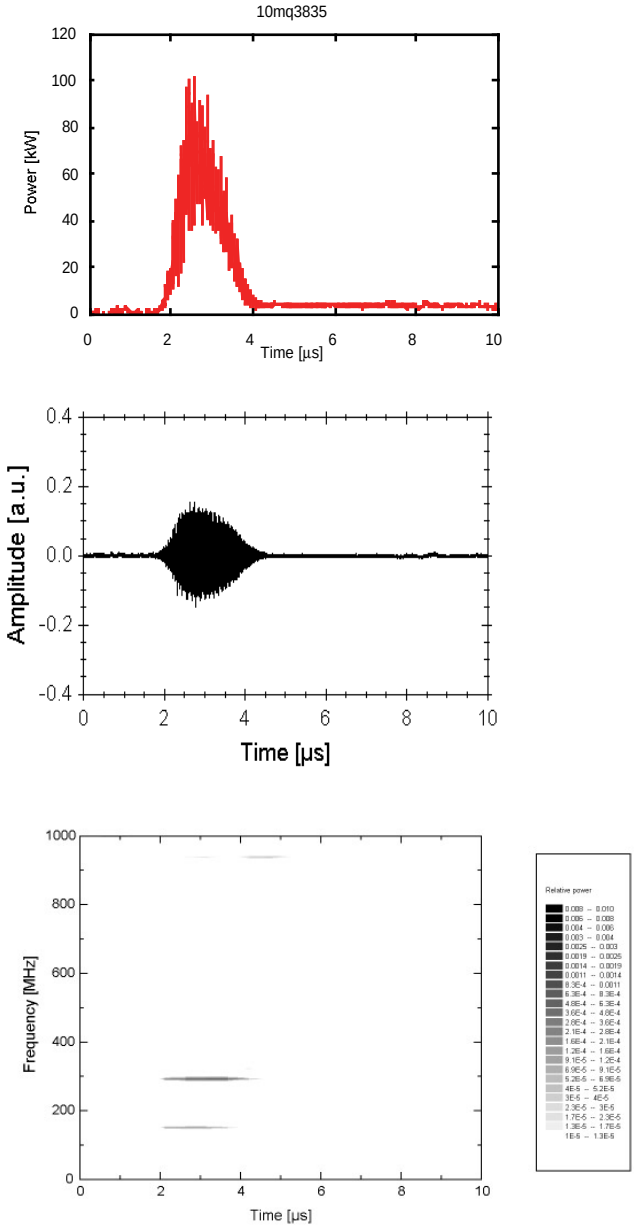

Figure 10. At the extreme edges of the parameter regime, e.g. a relatively low acceleration voltage only a short power pulse remains with a more or less broad frequency spectrum, with many frequencies 0.1–1 GHz away from the local oscillator frequency of 193.9 GHz. Acceleration voltage at start, 1.70 MV. Feedback coefficient, 0.7. Beam current, 6 A.

pressure vessel at earth potential for easy adjustments and fine tuning of the entire system. In this set-up, the decelerator and depressed collector are not installed yet, which means that the FEM pulse duration is limited.

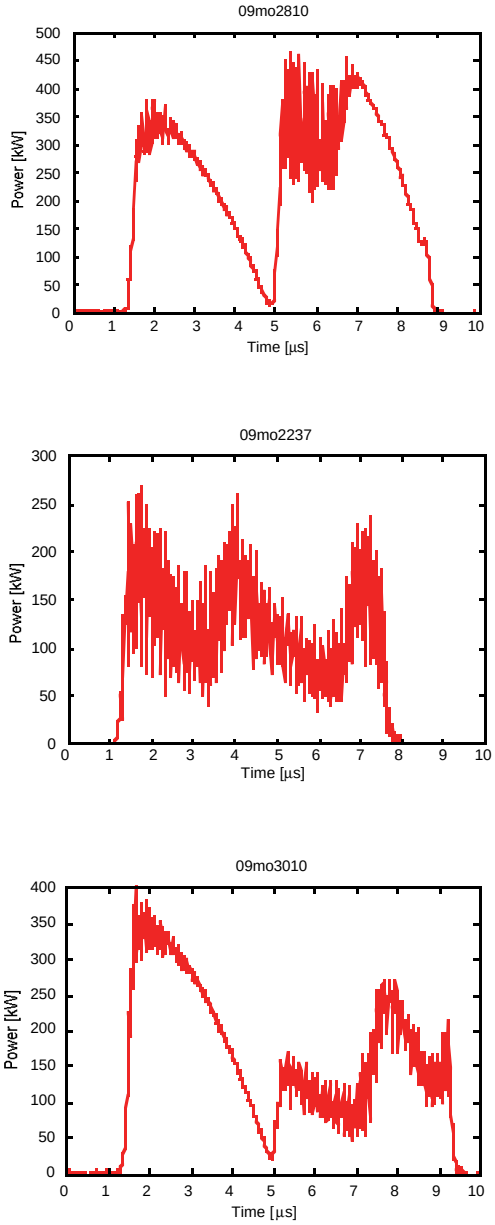

Figure 11. At very similar parameters (feedback coefficient, 0.7; beam current, 6 A), the output power can be completely different by just changing the start value of the acceleration voltage. Top, acceleration voltage at start, 1.754 MV; middle, acceleration voltage at start, 1.755 MV; bottom, acceleration voltage at start, 1.769 MV.

In October 1997, the fusion FEM, generated millimetre-wave power for the first time. During the first experiments the electron beam current was 6 A, which was enough to have strong amplification and to reach saturation for the present cavity settings (35% feedback power, 65% outcoupling).

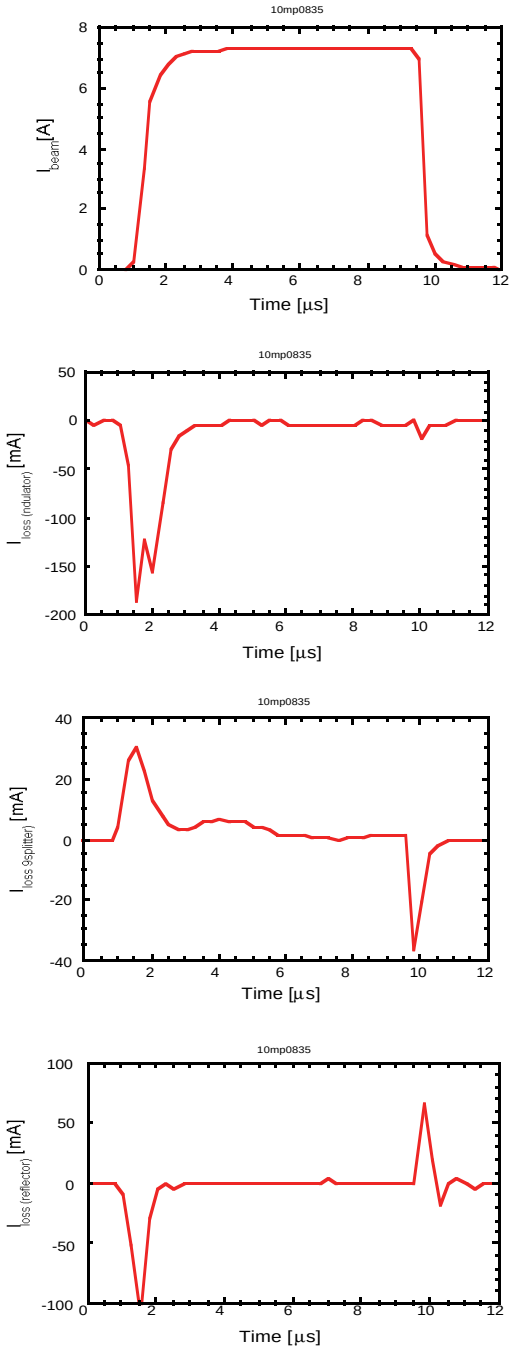

Figure 12. The measurement of the loss current shows very low losses. Apart from the beam current measured at the end of the beam line (dump), the losses at three positions in the beam line are also given. Apart from the peaks at the beginning and end of the pulse (which are partly induced currents on the waveguide wall instead of real beam losses and partly losses due to changing beam optics) the losses are extremely low.

At an acceleration voltage of 1.76 MV the millimetre-wave pulse starts after 3 μs and lasts for 3 μs, reaching a peak power level of 375 kW, see figure 6. Both output power and start-up time correspond well with simulation results.

In the present set-up (without electron beam recovery) the accelerating voltage drops rapidly during the pulse (1 kV A^{-1} of beam current per μs, so for 6 A this means 6 kV μs^{-1}, resulting in a frequency shift around 1.4 GHz μs^{-1}). Due to a bandwidth of the millimetre-wave cavity of just 4%, the pulse length is limited to a few microseconds, since the gain curve thus rapidly shifts across the cavity bandwidth. Consequently, the output power drops sharply and the pulse length is limited. At other parameter settings the output power drops as well, but at another (lower) frequency the power rises again after a few microseconds.

In the following figures the most interesting signals are given for different pulses: the acceleration voltage, the beam current and the millimetre-wave power as measured by a fast broadband detector. Furthermore, the millimetre-wave power is given as measured by a narrowband heterodyne system, with a local oscillator frequency of around 200 GHz. Also the FFT (fast Fourier transform) frequency spectrum is given. It can be seen that in one case (figure 6) the spectrum is very pure and in another case (figure 7), with very similar parameters (the acceleration voltage is about 6 kV higher) the spectrum is much broader. In the first case the output power grows to about 375 kW, while in the second case, most probably due to much more chaotic behaviour, the power remains substantially lower.

The highest power achieved so far is just over 700 kW (see figure 8). The power signal is peaked and drops sharply. A more or less flat output power signal can still be

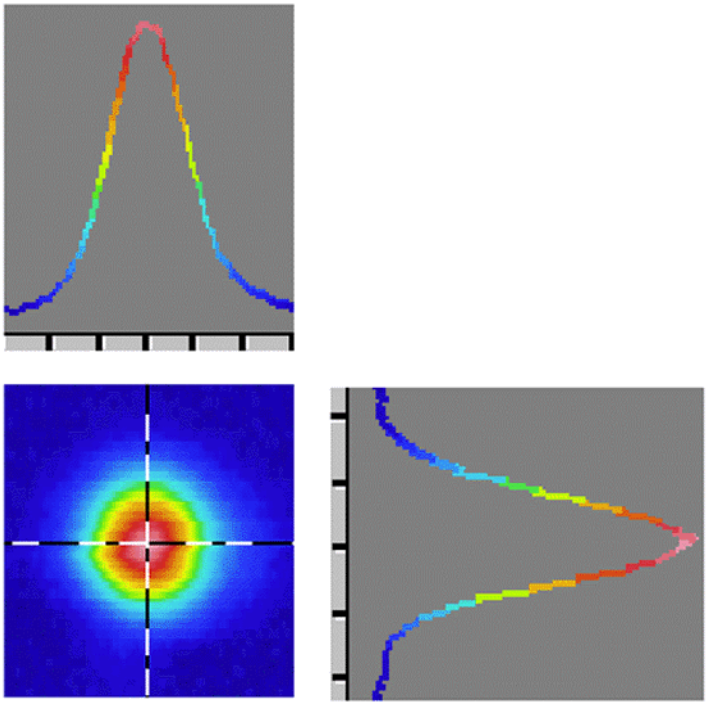

Figure 13. A measurement of the output millimetre-wave beam using an absorbing film under an angle of 45°. Measurements are performed by means of an infrared camera. A Gaussian profile can be seen in both directions. The profile was taken after a few pulses of 10 μs each at a repetition frequency of a 5–10 Hz having a peak power around 300 kW.

achieved if an increasing signal at a lower frequency is added to the usual decaying signal (see figure 9). A parameter scan has been performed for feedback coefficient, undulator drift gap and acceleration voltage. At the extreme edges of the parameter regime, e.g. a relatively low acceleration voltage only a short power pulse remains with a broad frequency spectrum, with many frequencies (see figure 10). In the case of very similar parameters the output power can be completely different by just changing the start value of the acceleration voltage, see figure 11. A Gaussian profile can be seen in both directions. In figure 12 a measurement is given with beam current losses as well.

A measurement of the output millimetre-wave beam profile was performed using an absorbing film (see figure 13). Measurements are performed by means of an infrared camera. A Gaussian profile was seen in both directions. The profile was taken after a few pulses of 10 μs each at a peak power around 300 kW and a repetition frequency of 5–10 Hz.

7. Conclusions

In the first phase of the project, experiments were performed in the inverse set-up. The entire beam line was tested successfully with extremely low-loss current, lower than 0.05%. This included the accelerating structure up to 2 MV level and the transport through the undulator and waveguide system. The first generation of millimetre waves was achieved in October 1997. The highest peak power measured so far is 700 kW at 200 GHz. This was achieved with a beam current of 8 A and an acceleration voltage of 1.77 MV. Output power, start-up time and frequency correspond well with simulation results. More experiments are on the way to try to understand the sensitivity of the output power, start-up time and frequency spectrum as a function of acceleration voltage, electron-beam radius, electron beam current, millimetre-wave feedback power and cavity tuning parameters. After the series of experiments in the inverse set-up, the equipment will be reinstalled in the final set-up as shown in figure 1. From that moment on, the pulse length can be extended up to 100 ms.

Acknowledgments

The authors are grateful to the many people who made very valuable contributions to this report: P Eecen, W Kooijman, G Kramer, G Land, J Plomp, A Putter, H Rietveld, F Wijnoltz and many others, Rijnhuizen. A Tulupov, A A Varfolomeev, S N Ivanchenkov, A S Khlebnikov, A V Smirnov and S V Tolmachev, Russian Research Centre, Kurchatov Institute Moscow, Russia. M Thumm, Forschungszentrum Karlsruhe, W Kasparek and D Wagner, Intitut für Plasmaforschung, Stuttgart, M Cattelino and G Miram, CPI/Varian, Palo Alto, CA, USA, P C T van der Laan, P van Deursen and J Wetzer, Technical University Eindhoven. This work was performed as part of the research programme of the association agreement of EURATOM and FOM with financial support from NWO and EURATOM.

References

[1] Makowski M A, Elio F and Loeser D 1998 *Proc. 10th Workshop on ECE and ECRH, EC10 (1997)* ed A J H Donne and A G A Verhoeven (Singapore: World Scientific) pp 549–59

[2] Urbanus W H *et al* 1998 *Proc. 10th Workshop on ECE and ECRH, EC10 (1997)* ed A J H Donne and A G A Verhoeven (Singapore: World Scientific) pp 497–506

[3] Caplan M, Nelson S, Kamin G, Antonsen T M, Levush B, Urbanus W H and Tulupov A V 1996 *Proc. 9th Workshop on ECE and ECRH, EC9 (1995)* ed J Lohr (Singapore: World Scientific) pp 333–41

[4] Schüller F C, Lopes Cardozo N J, Hogeweij G M D, de Baar M, Beurskens M N A, van der Meiden H J, Oomens A A M and RTP Team 1997 *Bull. Am. Phys. Soc.* **42** 1843
[5] de Loos M J and van der Geer S B 1996 *Proc. 5th Eur. Particle Accelerator Conf. (Sitges)* (Singapore: World Scientific) pp 1241–3
[6] Caplan M, Antonsen T M, Levush B, Tulupov A V and Urbanus W H 1995 *Nucl. Instrum. Methods* A **358** 174
[7] Tulupov A V, van der Wiel M J, Urbanus W H and Caplan M 1994 *Nucl. Instrum. Methods* A **341** 305
[8] Caplan M, Valentini M, van der Geer C A J and Urbanus W H 1996 *Nucl. Instrum. Methods* A **375** 91
[9] Valentini M, van der Geer C A J, Verhoeven A G A, van der Wiel M J, Urbanus W H and the FEM team 1997 *Nucl. Instrum. Methods* A **375** 409–16
[10] Eecen P J, Schep T J and Tulupov A V 1995 *Phys. Rev.* E **52** 5460
[11] Denisov G G and Shmelyov M Yu 1996 *Proc. 21st Int. Conf. on Infrared and Millimeter Waves (Berlin, BF3)* ed M von Ortenberg and H U Müller ISBN 3-00-000800-4
[12] Rivlin L A 1981 *Laser Focus* **17** 82
[13] Bongers W A *et al* 1998 *Proc. 10th Workshop on ECE and ECRH, EC10 (1997)* ed A J H Donne and A G A Verhoeven (Singapore: World Scientific) pp 507–14
[14] Bratman V L, Denisov G G, Savilov A V, Shmelyov M Yu, Urbanus W H and Verhoeven A G A 1998 *Proc. Free Electron Laser Conf. (Beijing, 1997)* (*Nucl. Instrum. Methods* to be published)